



**HAL**  
open science

## Chemical Characterization and Thermal Analysis of Recovered Liquid Crystals

Ana Barrera, Corinne Binet, Florence Danede, Jean-Francois Tahon, Baghdad Ouddane, Frédéric Dubois, Philippe Supiot, Corinne Foissac, Ulrich Maschke

► **To cite this version:**

Ana Barrera, Corinne Binet, Florence Danede, Jean-Francois Tahon, Baghdad Ouddane, et al.. Chemical Characterization and Thermal Analysis of Recovered Liquid Crystals. *Crystals*, 2023, Liquid Crystals and New Applications in Sensing and Sensors, 13 (7), pp.1064. 10.3390/cryst13071064 . hal-04310292

**HAL Id: hal-04310292**

**<https://hal.univ-lille.fr/hal-04310292>**

Submitted on 27 Nov 2023

**HAL** is a multi-disciplinary open access archive for the deposit and dissemination of scientific research documents, whether they are published or not. The documents may come from teaching and research institutions in France or abroad, or from public or private research centers.







L'archive ouverte pluridisciplinaire **HAL**, est destinée au dépôt et à la diffusion de documents scientifiques de niveau recherche, publiés ou non, émanant des établissements d'enseignement et de recherche français ou étrangers, des laboratoires publics ou privés.



Distributed under a Creative Commons Attribution 4.0 International License

## Article

# Chemical Characterization and Thermal Analysis of Recovered Liquid Crystals

Ana Barrera<sup>1</sup>, Corinne Binet<sup>1</sup>, Florence Danede<sup>1</sup>, Jean-François Tahon<sup>1</sup> , Baghdad Ouddane<sup>2</sup> , Frédéric Dubois<sup>3</sup> , Philippe Supiot<sup>1</sup> , Corinne Foissac<sup>1</sup>  and Ulrich Maschke<sup>1,\*</sup> 

- <sup>1</sup> Unité Matériaux et Transformations (UMET), UMR 8207, CNRS, INRAE, Centrale Lille, Université de Lille, 59000 Lille, France; ana-luisa.barrera-almeida@univ-lille.fr (A.B.); corinne.binet@univ-lille.fr (C.B.); florence.danede@univ-lille.fr (F.D.); jean-francois.tahon@univ-lille.fr (J.-F.T.); philippe.supiot@univ-lille.fr (P.S.); corinne.foissac@univ-lille.fr (C.F.)
- <sup>2</sup> Laboratoire de Spectroscopie Pour les Interactions, la Réactivité et l'Environnement (LASIRE), UMR 8516, Université de Lille, 59000 Lille, France; baghdad.ouddane@univ-lille.fr
- <sup>3</sup> Unité de Dynamique et Structure des Matériaux Moléculaires, (UDSMM), UR 4476, Université du Littoral Côte d'Opale, 59379 Dunkerque, France; frederic.dubois@univ-littoral.fr
- \* Correspondence: ulrich.maschke@univ-lille.fr; Tel.: +33-3-20-33-63-81

**Abstract:** Chemical, structural, and thermal properties of recovered nematic Liquid Crystal (LC) mixtures were investigated by applying several analytical techniques. A large quantity (65,700) of End-Of-Life (EOL) Liquid Crystal Display (LCD) screens were used to extract these LC blends. The studied EOL-LCD screens were heterogeneous in nature, particularly due to their different brands, production years, and dimensions. The collected TV and computer screens, as well as tablets, presented an average diagonal size of 24 inches. Chemical characterization revealed that the recovered compounds present typical chemical structures of LC molecules by the simultaneous presence of aliphatic chains and aromatic and polar groups. POM observations of these samples exhibited Schlieren and marble-like textures at room temperature, which are typical of nematic LCs. Moreover, thermal characterization and thermo-optical analysis showed that these LC mixtures displayed a broad nematic phase between  $-90\text{ }^{\circ}\text{C}$  and  $+70\text{ }^{\circ}\text{C}$ .

**Keywords:** End-Of-Life Liquid Crystal Displays; nematic liquid crystals; recycling; chemical and thermal properties



**Citation:** Barrera, A.; Binet, C.; Danede, F.; Tahon, J.-F.; Ouddane, B.; Dubois, F.; Supiot, P.; Foissac, C.; Maschke, U. Chemical Characterization and Thermal Analysis of Recovered Liquid Crystals. *Crystals* **2023**, *13*, 1064. <https://doi.org/10.3390/cryst13071064>

Academic Editors: Shigeyuki Yamada and Vladimir Chigrinov

Received: 21 April 2023  
Revised: 26 June 2023  
Accepted: 28 June 2023  
Published: 6 July 2023



**Copyright:** © 2023 by the authors. Licensee MDPI, Basel, Switzerland. This article is an open access article distributed under the terms and conditions of the Creative Commons Attribution (CC BY) license (<https://creativecommons.org/licenses/by/4.0/>).

## 1. Introduction

The omnipresence of technologies in modern societies leads to their excessive consumption and, therefore, their overproduction. Televisions, laptops, cell phones, tablets, etc. reflect the increasing availability of screens and raise many questions about the treatment of the electronic waste they generate. Indeed, such waste is not biodegradable and contains substances that are harmful to the environment [1–3]. In addition, the progressive complexity of electronic devices complicates their recycling. It is therefore essential to find a suitable treatment for these devices in order to recover the valuable materials they contain and give them a second life [4,5]. In this context, the main purpose of our research concerns the recovery of liquid crystals (LCs) present in end-of-life (EOL) LCD screens.

In the past, environmental studies on LCD screens were mainly concentrated on investigations to detect heavy metals, such as Cr, Pb and Hg, among others. Several reports are now available in recent literature, demonstrating the hazardousness of LC mixtures and classifying many of them as toxic Persistent Organic Pollutants (POPs) [6–9]. Considering more than 300 LC compounds, Li et al. applied the criteria proposed by the US Environmental Protection Agency (USEPA) and discovered that more than 90% of these LCs have the potential to persist and bioaccumulate (P&B) after entering the environment [6]. Su et al. revealed that 87 out of 362 investigated LC molecules from indoor dust samples

were identified as P&B chemicals [7]. Further studies were carried out to determine the exposure of workers to hazardous LC mixtures from dismantling operations in an e-waste recycling industrial park. The high-resolution mass spectrometry (HRMS) method was applied to detect mainly fluorinated biphenyl- and bicyclohexyl-derivatives [8]. In 2022, Su et al. established a database of 1173 LCs; these molecules were used to identify their presence in 33 sediment samples, using GC-QTOF/MS techniques [9].

The above-mentioned considerations are strong motivations to investigate the possibility of closed-loop remediation processes for LC molecules. Recycling LCs is a challenging task because LCD screens, depending on their dimension, type, year of production, etc., contain a mixture of a large number of different LC molecules. It should be mentioned that, to protect their production secrets and to stand out from the competition, LCD panel manufacturers add a whole series of additives and use different LCs blends for each of their technologies. The main LCD screen types are twisted nematic (TN), in-plane switching (IPS), and Vertical Alignment (VA). Each native LC mixture used in one single LCD screen is composed of about 20 or more LC molecules (mainly nematic ones), together with a certain number of additives. Each manufacturer uses a specific native LC mixture according to the type of screen and the technology to be developed. Since this information is not available (trade secret), the LC composition of the corresponding native LC mixture is unknown. This implies that, after recovery of LC molecules from various EOL-LCD screens, a complex mixture of a large number of different LCs and other molecules will be obtained. This means that it is not appropriate to investigate specific native LC mixtures in order to compare their chemical and physical properties with those from the collected EOL-LCD screens. Since the preservation of the properties of a recycled product remains crucial for its reuse, an in-depth characterization of chemical, thermal, optical, and dielectric properties of the recovered LC mixtures needs to be carried out.

A previous report considered the chemical and thermal characterization of four LC mixtures gathered from 35 EOL-LCD screens, which were older than five years [10]. These LC blends were analyzed without supplementary purification steps. In the present work, the previous investigation was extended to the recovery and analysis of LC molecules extracted from a total of about 65,700 EOL-LCD screens, which were accumulated on an industrial recycling line during a period of one year. The recovered LC compounds were gathered in the form of three mixtures, following the collection periods. The obtained LC blends underwent several purification procedures, including distillation, filtration, and chromatography.

In this report, much consideration will be given to the chemical characterization and thermal analysis of the recovered LC blends, since they represent unique and new features as unknown mixtures, which were not considered until now in the literature. Indeed, many single molecules included in these blends can be qualitatively identified by their CAS registry number. On the other hand, in order to be able to evaluate the possibility to reuse the recovered LC mixtures as new products for the original or a new application, requirements specification must be performed. In particular, physico-chemical properties of purified LC mixtures will be compared with those from non-purified blends. Furthermore, it should be mentioned that the dielectric characteristics of these systems have already been described in the literature [11–13].

Fourier Transform Infrared Spectroscopy (FTIR), as well as  $^1\text{H}$ -Nuclear Magnetic Resonance ( $^1\text{H}$ -NMR), techniques will be employed to investigate the spectroscopical properties of the LC molecules present in the complex mixtures. Samples will also be analyzed by gas chromatography, coupled with a mass spectrometer (GC-MS), a technique which should allow chromatographic separation and identification of individual LC molecules from the blend, in order to obtain qualitative and quantitative information about these compounds. Thermal and thermo-optical properties of the recovered LC mixtures will be studied essentially by Thermogravimetry (TGA), Differential Scanning Calorimetry (DSC), and by Polarized Optical Microscopy (POM), coupled with a heating/cooling stage.

In particular, attention will be paid to the investigation of the nature of the LC phase, as a function of temperature. The dominant LC phase generally found in LCD screens is the nematic phase [14–16]. This phase is defined by an order of orientation of the LC molecules, without specific positions in space. The molecules tend to align themselves parallel to each other; their direction is symbolized by the unit director vector of the medium noted  $n$  [17,18]. In display applications, mixtures of LC molecules present an eutectic phase behavior in order to obtain a stable nematic phase over a wide temperature range [19]. Analysis of the recovered LC blends by POM and DSC will allow elucidation of this important feature.

## 2. Materials and Methods

### 2.1. Materials

Currently, the company Envie<sup>2</sup>E, based in the surroundings of Lille (France), operates a processing line aiming to recycle EOF-LCD screens by manual, orderly dismantling techniques. This procedure allows for the removal of different valuable items from EOF-LCD screens, which can then be redirected to the adapted recycling sectors. In addition, the company has developed an extraction line for the recovery of LCs from EOF-LCD panels. These organic molecules were recuperated by exposing the previously opened LCD panels to an organic solvent bath. The ultrasound-assisted extraction (UAE) technique has been applied to increase the extraction yield. This unique process and its details are the subject of a patent filed by Maschke et al. [20].

From this extraction line, three samples were collected, corresponding to three extraction periods spread over one year: from the 1st to the 4th month (NP-1), from the 5th to the 8th month (NP-2), and from the 9th to the 12th month (NP-3). These LC blends were accumulated from about 65,700 LCD panels of diverse brands, dimensions, types (televisions, monitors, laptops, and tablets), technologies, manufacture dates, etc.

The LC blends recovered from the extraction line contain a mixture of a large number of different LC and other molecules used by the different manufacturers, with the organic solvent employed for extraction, as well as organic and inorganic impurities. These samples presented a black coloration, which is not representative of pure nematic LC mixtures (Figure 1). A multi-step purification process was therefore carried out in order to remove a maximum of impurities, before thinking about a possible reuse of these recycled LCs. The different purification steps are displayed in Figure 1.

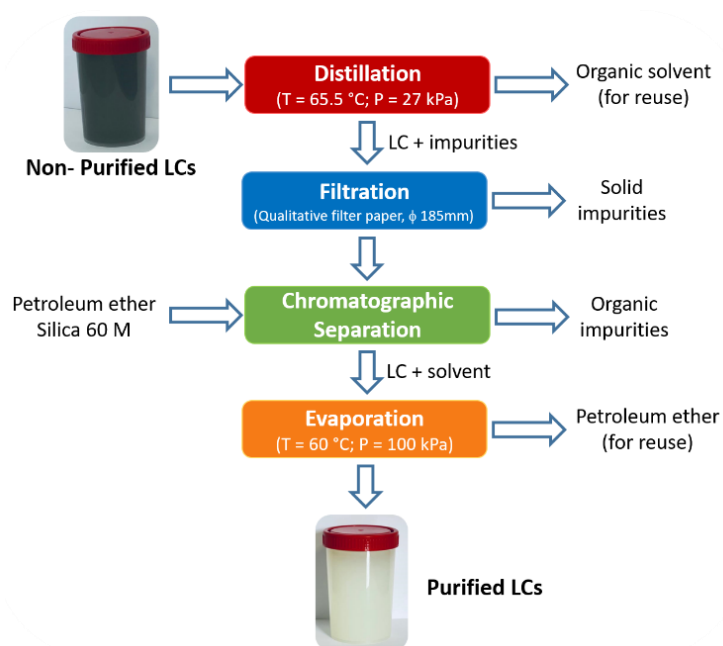


**Figure 1.** Purification steps of the LC mixtures collected from the industrial extraction line.



The purification process starts with a vacuum distillation (applying a reduced pressure of 27 kPa at  $T = 65\text{ }^{\circ}\text{C}$ ) to remove the organic solvent used during the industrial extraction process. The distilled solvent was collected to be reused in the extraction line at ENVIE<sup>2</sup>E. As a result of the distillation step, solid particles were found, together with the LC containing blends. Consequently, a filtration of these impurities was performed using a funnel and a qualitative filter paper (Whatman<sup>®</sup>, Global Life Sciences Solutions, MA, USA; Grade 287 1/2, diameter 185 mm). Afterwards, a separation by column chromatography was conducted in order to enhance the purity of the LC samples. Using this technique, silica (SiO<sub>2</sub> 60 M, 0.04–0.063 mm, Macherey-Nagel, Düren, Germany) was employed as the stationary phase to retain impurities, and petroleum ether (40–60 °C fraction, VWR, Rosny-sous-Bois, France) was used as the mobile phase to recover the LCs. Finally, evaporation of the used solvent was performed and the purified LC mixtures were collected. These obtained mixtures presented a “milky white” appearance, typical of a nematic phase containing molecules possessing mesogenic moieties.

## 2.2. Methods

### 2.2.1. Chemical Characterizations

The molecular structures of the non-purified and purified LC mixtures were investigated with a Perkin Elmer FTIR Frontier spectrometer (Perkin Elmer, Shelton, CT, USA) in the range from 4000 to 400  $\text{cm}^{-1}$ , applying a spectral resolution of 4  $\text{cm}^{-1}$ . The number of accumulated scans was 16. All FTIR studies were performed in the ATR (Attenuated Total Reflectance) mode using a diamond prism. Then, <sup>1</sup>H proton NMR analyses were performed at room temperature with a 300 MHz Bruker Avance III HD spectrometer (Bruker, San Jose, CA, USA), using tubes of 5 mm diameter. The LC mixtures were dissolved in chloroform (CDCl<sub>3</sub>) as a deuterated solvent, exhibiting a high purity (~99.8%, Eurisotop, Saint-Aubin, France). The resulting <sup>1</sup>H NMR spectra were analyzed with Masternova software (version 12.0.4).

The non-purified and purified LC mixtures were analyzed by gas chromatography, coupled with a mass spectrometer (GC-MS) from Perkin Elmer (Perkin Elmer, Shelton, CT, USA). The setup was equipped with a Clarus 680 gas chromatograph, a 30 m × 0.25 mm Elite-XLB capillary column with a 0.10  $\mu\text{m}$  film thickness, coupled to a Clarus 600T mass detector equipped with a quadrupole mass analyzer (QSM) (Perkin Elmer, Shelton, CT, USA). The carrier gas used was pure helium, with a constant flow rate of 1.5 mL/min. Before injection of the samples, the LC mixtures were diluted with tetrahydrofuran (THF) to obtain a concentration of 1 g/L. Samples were introduced to the GC injection system using a microsyringe (0.6  $\mu\text{L}$  volume) when the oven temperature reached 300 °C. The initial program temperature was set at 120 °C, followed by a 10 °C/min ramp to 300 °C, and a 30 min isotherm at the latter temperature.

A purified LC mixture was also analyzed using Laser Desorption Ionization (LDI), coupled to High Resolution Fourier-Transform Ion Cyclotron Resonance Mass Spectrometry (HR-FT-ICR-MS). External calibration of the HRMS instrument was performed using red phosphorus (Sigma Aldrich-Merck, Saint Quentin Fallavier, France). A small volume of about 1  $\mu\text{L}$  of the diluted LCs (1:10 in Acetone) was deposited on a commercially available 384-well stainless-steel target. After drying at room temperature, a homogenous thin layer was obtained. A Solari XR FT-ICR-MS (Bruker Daltonics GmbH & Co. KG, Bremen, Germany), equipped with a 9.4-T magnet (Magnex Scientific, Oxfordshire, UK), was operated in positive-ion mode at a resolution of around 530,000 @  $m/z$  400 with an 8 M transient. To obtain an acceptable signal-to-noise ratio, 50 scans were accumulated. Additionally, the laser spot was not fixed at one position, but random walk was employed with a typical border width of 1000  $\mu\text{m}$ . For ionization, the third harmonic of a neodymium-YAG laser (355 nm) (provided by Bruker Daltonics GmbH & Co. KG, Bremen, Germany) was used. The settings were optimized as follows: “35% laser power”, “small spot size” (corresponding to 80–100  $\mu\text{m}$ ), 100 pulses per laser shot, and a frequency of 200 Hz. Data visualization was performed with Bruker Compass DataAnalysis 5.0 SR1 software, and

molecular formula assignments were performed with Small Molecule Accurate Recognition Technology (SMART).

Inorganic impurities (ions) present in the non-purified and purified LC mixtures were identified by the inductively coupled plasma atomic emission. The samples were first mixed with aqua regia ( $\text{HNO}_3 + 3 \text{HCl}$ ) to conduct a liquid-liquid extraction. The resulting inorganic phase was analyzed using an Agilent 5110 ICP-AES spectrometer (dual view SVDV, Santa Clara, CA, USA). The device was equipped with an inert Sturmun-Master (PTFE) spray chamber and a V-Groove pneumatic nebulizer (Santa Clara, CA, USA). The plasma power was set at 1.2 kW, and an argon flow rate of 1.5 L/min was used.

### 2.2.2. Thermo-Optical and Thermal Characterizations

In order to determine the thermal stability of the LCs mixtures, measurements were performed on a thermogravimetric analyzer from TA Instruments (New Castle, DE, USA) (Q5000). The analyses were conducted in a temperature range between 20 and 800 °C, with a heating rate of 10 °C/min, under a nitrogen gas flow of 50 mL/min. Differential scanning calorimetry (DSC) was performed using a DSC calorimeter from TA Instruments (Q10), equipped with a cooling system. The LC mixtures were inserted into hermetic standard aluminum DSC capsules. Sample masses were about 2.5 mg. The samples were subjected to three consecutive heating and cooling cycles in a temperature range between −150 and 100 °C under continuous nitrogen flow, applying a rate of 10 °C/min.

The mesophase type, phase transitions, and clearing temperatures of LC mixtures were observed using an Olympus BX41 POM (Olympus Corporation, Tokyo, Japan), equipped with a Linkam LTS 350 (Linkam Ltd., Surrey, UK) heating and cooling stage, connected to a camera and a computer with photo recording software. A drop of LC mixture was placed between two clean glass slides, without preferential alignment of the sample. First, LCs samples were cooled down from room temperature to −110 °C at a rate of 10 °C/min, followed by a 5 min isotherm at this temperature to stabilize the sample, and then slowly heated at 5 °C/min to 100 °C. Finally, a second cooling process was carried out from 100 °C to −110 °C at 10 °C/min. Pictures were taken from the sample morphology during the cooling and heating cycles.

### 2.2.3. Structural Properties

In order to identify the phase behavior of the LC mixtures, Wide-Angle X-ray Scattering (WAXS) measurements were carried out using a Xeuss 2.0 instrument from Xenocs (Holyoke, MA, USA). This apparatus was equipped with a Cu micro source ( $\lambda = 1.5418 \text{ \AA}$ ) and a Pilatus 200K 2D detector (Rigaku Oxford diffraction, Wroclaw, Poland), placed at a distance of 140 mm from the sample. The exposure time employed was 120 s and experiments were conducted in a cooling–heating–cooling process (following the same thermal cycles as already described for the POM analysis).

The LC mixtures were inserted into quartz glass capillaries (Hilgenberg, Malsfeld, Germany) with an internal diameter of 1.5 mm and a length of 80 mm. The capillaries were then sealed with a two-component epoxy adhesive.

## 3. Results and Discussions

### 3.1. Chemical Properties

#### 3.1.1. FTIR Analysis

Figure 2 shows the FTIR spectra obtained for three non-purified LC mixtures (NP-M1, NP-M2, and NP-M3) and for three purified LC mixtures (P-M1, P-M2, and P-M3) in the 4000–400  $\text{cm}^{-1}$  region.

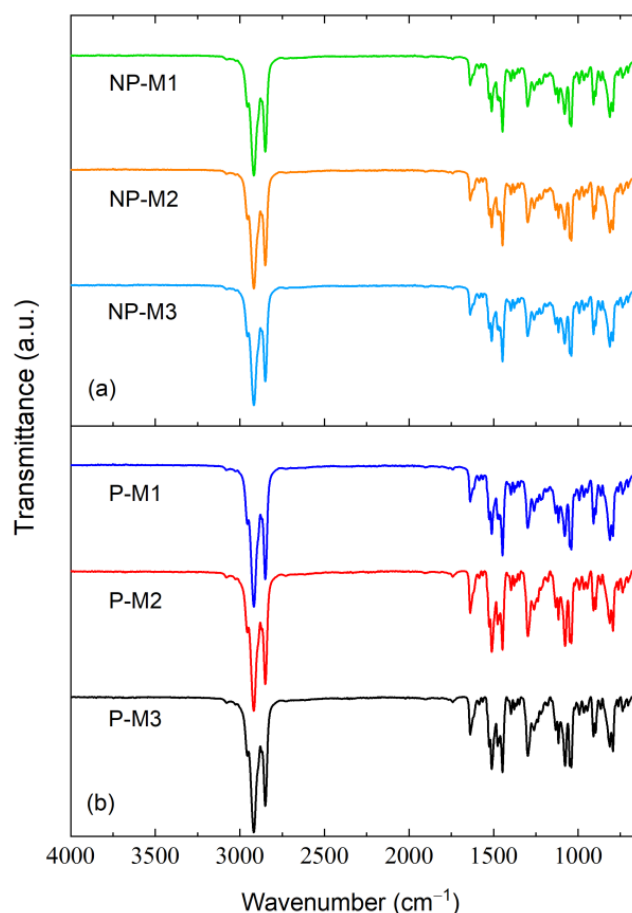


**Figure 2.** (a) FTIR spectra of the three non-purified LC mixtures (NP-M1, NP-M2 and NP-M3) and (b) of the three purified LC mixtures (P-M1, P-M2 and P-M3).

The spectra obtained for the purified LC mixtures appear to be quite identical to those found for non-purified mixtures: the position of the vibration bands and their relative intensities were found to be similar. Consequently, the same functional groups might be present in the studied mixtures. It was noticed that the sensitivity of the FTIR technique does not allow detecting any difference between purified and non-purified samples.

The spectra in Figure 2 show two well-differentiated areas with several bands of medium and strong intensities. These bands can be attributed to the rigid core (aromatic groups) and to the flexible part of the LC molecules (aliphatic chains).

For all spectra shown in Figure 2, two strong intensity bands could be revealed between 2950 and 2800  $\text{cm}^{-1}$ , corresponding to the vibrational modes of the C-H bonds of the aliphatic chains. Between 1700 and 500  $\text{cm}^{-1}$ , a group of bands was found, confirming the presence of:

- elongation vibrations of the aromatic C=C double bond (1600–1500  $\text{cm}^{-1}$ );
- elongation vibrations of the C-F bond; fluorinated compounds (1400–1000  $\text{cm}^{-1}$ );
- elongation vibrations of the C-N and C-O bonds; aromatic amines and esters (1340–1250  $\text{cm}^{-1}$ );
- deformation vibrations of C=C double bonds; alkenes (cis, trans . . . ) (1000–650  $\text{cm}^{-1}$ );
- out-of-plane deformation vibrations of the =C-H bond of an adjacent hydrogen on an aromatic ring (910  $\text{cm}^{-1}$ );
- out-of-plane deformation vibrations of the =C-H bond of two adjacent hydrogens on an aromatic ring (815  $\text{cm}^{-1}$ ).

It should be mentioned that the characteristic band attributed to the cyano group (C≡N), generally located between 2200 and 2300  $\text{cm}^{-1}$ , was not detected in the LC mixtures

studied in this report. This band can be found in some commercial nematic LC mixtures, for example, in the case of E7 (formally from Merck), a mixture of cyanobiphenylene compounds [21]. For the recycled LC mixtures, this functional group was not visible on the spectrum because these cyano-biphenyl-containing molecules were not used any more, or only in very weak quantities, in the LC blends employed in the accumulated EOL-LCD screens. Moreover, the sensitivity of the FTIR technique does not allow for detection of the cyano group when present at weak concentrations.

### 3.1.2. NMR Analysis

The  $^1\text{H}$  proton NMR analysis of the non-purified and purified LC mixtures was performed to corroborate the FTIR results, in order to elucidate the molecular structure of LC mixtures. The collected spectra are shown in Figure 3. All spectra were recorded at room temperature and under identical conditions, i.e., using the same deuterated solvent and the same sample concentration.

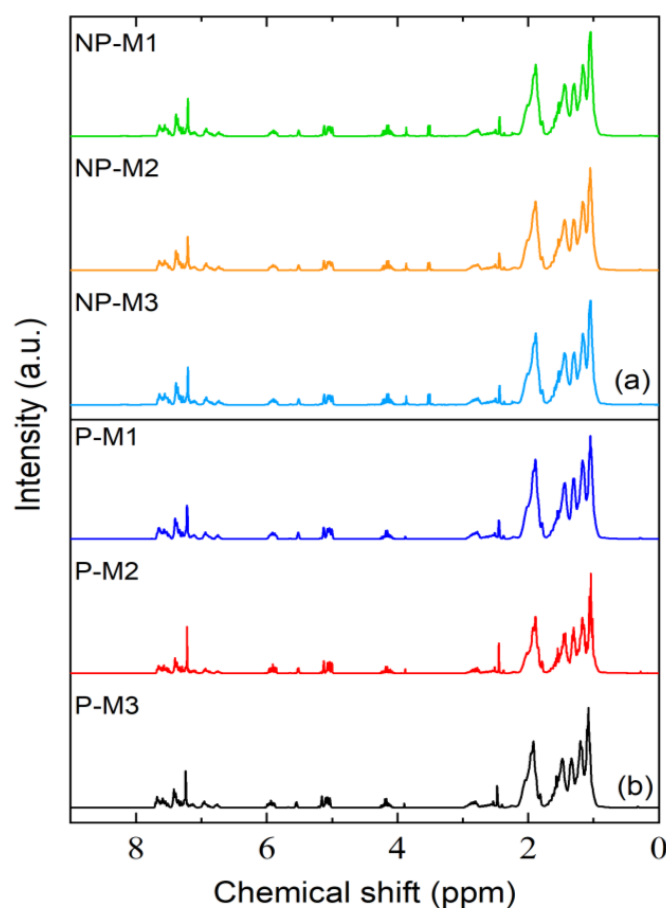


**Figure 3.** (a)  $^1\text{H}$  proton NMR spectra of the three non-purified LC mixtures (NP-M1, NP-M2, and NP-M3) and (b) of the three purified LC mixtures (P-M1, P-M2, and P-M3) at room temperature.

### 3.1.3. GC-MS and HRMS Analysis

GC-MS analysis was performed to separate the recycled LC mixtures and identify their components. Figure 4 shows the chromatograms obtained for non-purified and purified LC mixtures.

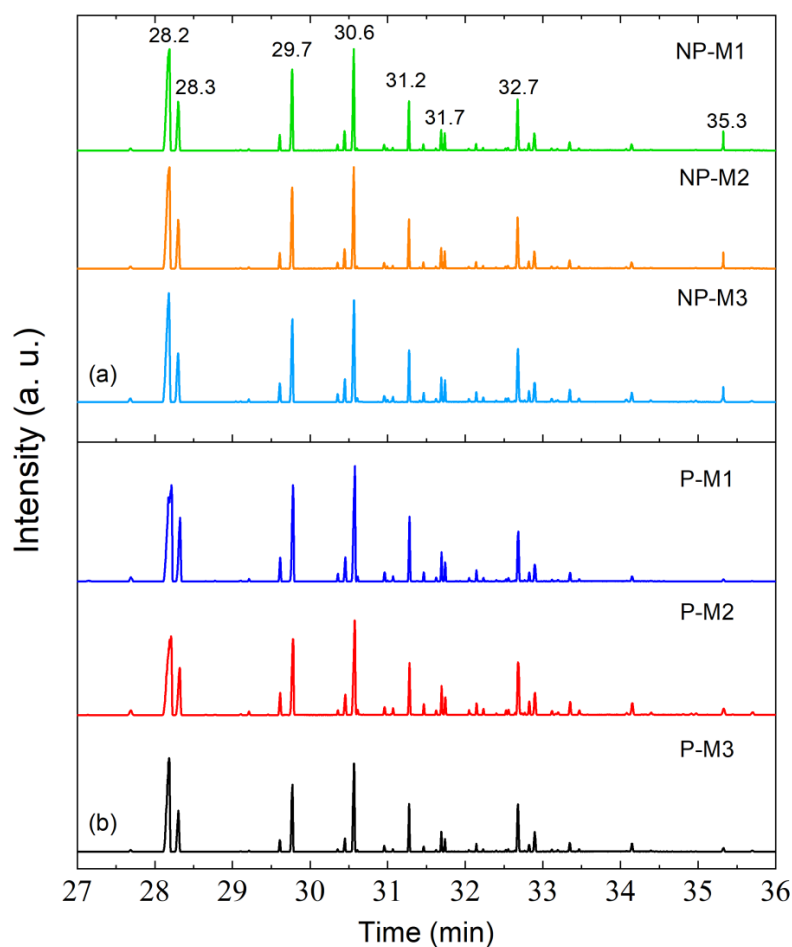


**Figure 4.** (a) GC chromatograms of the three non-purified LC mixtures (NP-M1, NP-M2, and NP-M3) and (b) of the three purified LC mixtures (P-M1, P-M2, and P-M3). The numbers (28.2, 28.3, . . . ) correspond to the retention times of the most intense peaks reproduced in Table 1.

The chromatograms collected for the three non-purified LC mixtures, as well as for the three purified LC mixtures, were found to be almost identical to each other. The non-purified mixtures show a low-intensity peak at ~35.3 min that hardly appeared in the purified mixtures. The chemical structures of some molecules corresponding to the most intense peaks in the chromatograms were estimated by exploitation of the mass spectrometry results, applying an MS reference database. MS data obtained by GC-MS analysis represent integer masses. In general, there are many chemical structures with different compositions, even if the integer mass is the same. Therefore, in order to obtain integer mass peaks, high-resolution MS (HRMS) measurements were performed on a purified LC mixture, using the FT-ICR-MS technique. The HRMS results, in terms of obtained and calculated exact masses of putative structures, were reported (see Table 1). A good match between these data were obtained, confirming thus the presence of these molecules in the LC mixture.

According to Table 1, nearly all identified molecules show the typical chemical structure of LCs, as can be revealed by the simultaneous presence of rigid (aromatic rings, . . . ) and flexible (aliphatic chains, . . . ) parts covalently bound in the same compound. Moreover, one notes the presence of polar groups leading to the existence of an electric dipole moment. The identification of some peaks was not possible, due to the absence of molecular structures in the database used. In some cases, the suggestions provided by the database did not show theoretical spectra similar to those obtained, and presented weak probability (<30%).

**Table 1.** Chemical structures of some molecules present in the purified LC mixtures. CAS RN corresponds to the registry number from Chemistry Abstract Service.

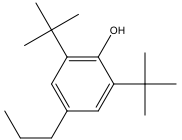
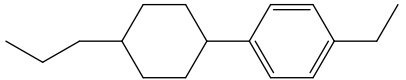
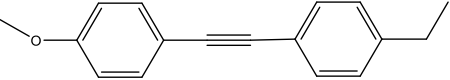
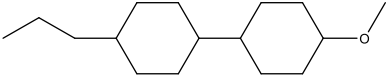
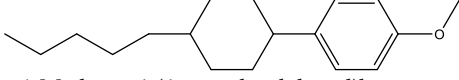
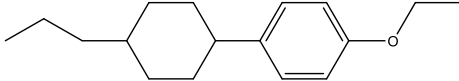

CAS RN	Molecular Structure and Name	GC-MS: Retention Time (min)	HRMS: Exact Masses ( $m/z$ ) Obtained/ Calculated	Molecular Formula
4973-24-4	 2,6-di-tert-butyl-4-propylphenol	27.69	248.2138/ 248.2138	C <sub>17</sub> H <sub>28</sub> O
82991-47-7	 1-Ethyl-4-(4-propylcyclohexyl)benzene	28.21	230.2033/ 230.2033	C <sub>17</sub> H <sub>26</sub>
63221-88-5	 1-(4-Ethylphenyl)-2-(4-methoxyphenyl)acetylene	28.32	236.1201/ 236.1200	C <sub>17</sub> H <sub>16</sub> O
97398-80-6	 4-Methoxy-4'-propyl-1,1'-bi(cyclohexyl)	29.61	238.2296/ 238.2296	C <sub>16</sub> H <sub>30</sub> O
84952-30-7	 1-Methoxy-4-(4-pentylcyclohexyl)benzene	29.78	260.2139/ 260.2138	C <sub>18</sub> H <sub>28</sub> O
80944-44-1	 4-(trans-4-Propylcyclohexyl)-1-ethoxy-benzene	30.36	246.1982/ 246.1983	C <sub>17</sub> H <sub>26</sub> O
129738-34-7	 4-Pentyl-4'-vinyl-1,1'-bi(cyclohexyl)	30.45	262.2657/ 262.2658	C <sub>19</sub> H <sub>34</sub>



Table 1. Cont.

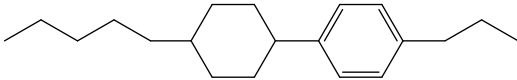
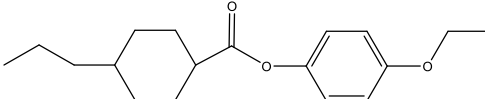
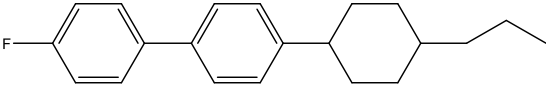
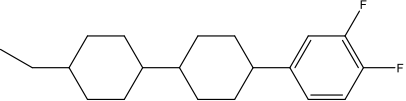
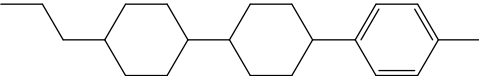
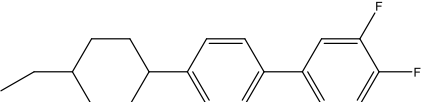
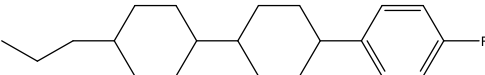
CAS RN	Molecular Structure and Name	GC-MS: Retention Time (min)	HRMS: Exact Masses ( $m/z$ ) Obtained/Calculated	Molecular Formula
82991-48-8	 1-(4-Pentylcyclohexyl)-4-propylbenzene	30.58	272.2501/ 272.2502	C <sub>20</sub> H <sub>32</sub>
67589-39-3	 4-ethoxyphenyl 4-propylcyclohexane-1-carboxylate	30.56	290.1880/ 290.1880	C <sub>18</sub> H <sub>26</sub> O <sub>3</sub>
87260-24-0	 4-Fluoro-4'-(4-propylcyclohexyl)-1,1'-biphenyl	30.96	296.1938/ 296.1939	C <sub>21</sub> H <sub>25</sub> F
118164-50-4	 4-(4'-ethyl [1,1'-bicyclohexane]-4-yl)-1,2-difluorobenzene	31.07	306.2156/ 306.2157	C <sub>20</sub> H <sub>28</sub> F <sub>2</sub>
84656-75-7	 Benzene, 1-methyl-4-(4'-propyl[1,1'-bicyclohexyl]-4-yl)-	31.28	298.2658/ 298.2658	C <sub>22</sub> H <sub>34</sub>
134412-18-3	 4'-(4-Ethylcyclohexyl)-3,4-difluoro-1,1'-biphenyl	31.46	300.1688/ 300.1688	C <sub>20</sub> H <sub>22</sub> F <sub>2</sub>
82832-27-7	 4-(4-Fluoro-phenyl)-4'-propyl-1,1'-bicyclohexyl	31.62	302.2407/ 302.2408	C <sub>21</sub> H <sub>31</sub> F

Table 1. Cont.

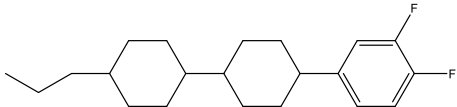
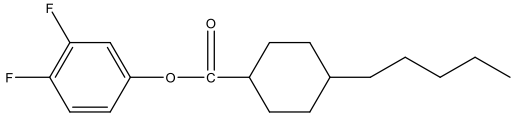
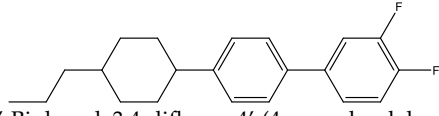
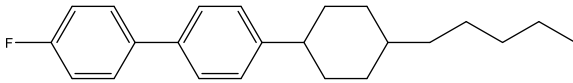
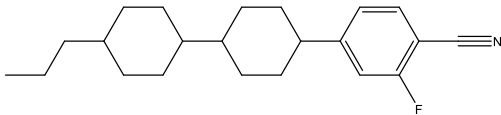
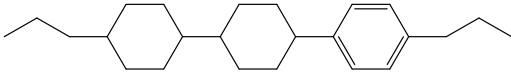
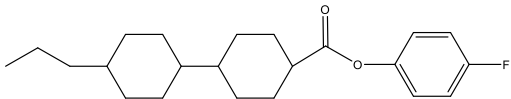
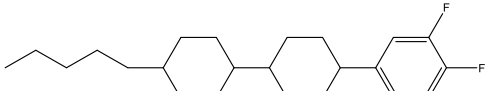
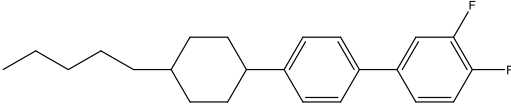
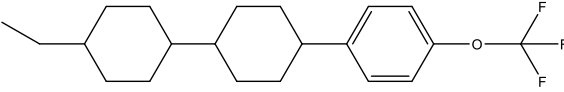
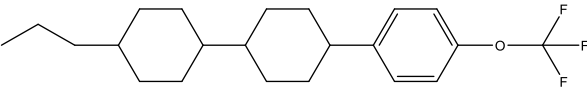
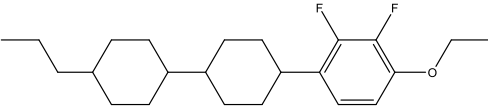
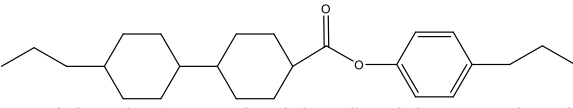
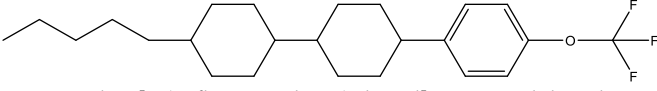
CAS RN	Molecular Structure and Name	GC-MS: Retention Time (min)	HRMS: Exact Masses ( $m/z$ ) Obtained/Calculated	Molecular Formula
82832-57-3	 4-(3,4-Difluorophenyl)-4'-propyl-1,1'-bi(cyclohexyl)	31.69	320.2315/ 320.2314	C <sub>21</sub> H <sub>30</sub> F <sub>2</sub>
89203-80-5	 3,4-difluorophenyl 4-pentylcyclohexane-1-carboxylate	31.74	310.1744/ 310.1743	C <sub>18</sub> H <sub>24</sub> F <sub>2</sub> O <sub>2</sub>
85312-59-0	 1,1'-Biphenyl, 3,4-difluoro-4'-(4-propylcyclohexyl)-	32.05	314.1843/ 314.1844	C <sub>21</sub> H <sub>24</sub> F <sub>2</sub>
81793-59-1	 4-Fluoro-4'-(4-pentylcyclohexyl)-1,1'-biphenyl	32.23	324.2251/ 324.2251	C <sub>23</sub> H <sub>29</sub> F
93743-04-5	 4-(4'-ethyl-[1,1'-bi(cyclohexan)]-4-yl)-2-fluorobenzonitrile	32.52	327.2359/ 327.2360	C <sub>22</sub> H <sub>30</sub> FN
84656-77-9	 4-propyl-4'-(4-propylphenyl)-1,1'-bi(cyclohexane)	32.55	326.2973/ 326.2973	C <sub>24</sub> H <sub>38</sub>
81701-13-5	 4-fluorophenyl 4-(4-propylcyclohexyl)cyclohexanecarboxylate	32.63	346.2309/ 346.2308	C <sub>22</sub> H <sub>31</sub> FO <sub>2</sub>

Table 1. Cont.

CAS RN	Molecular Structure and Name	GC-MS: Retention Time (min)	HRMS: Exact Masses ( $m/z$ ) Obtained/Calculated	Molecular Formula
118164-51-5	 4-(3,4-Difluorophenyl)-4'-pentyl-1,1'-bi(cyclohexyl)	32.68	348.2625/ 348.2626	C <sub>23</sub> H <sub>34</sub> F <sub>2</sub>
134412-17-2	 1,1'-Biphenyl, 3,4-difluoro-4'-(4-pentylcyclohexyl)	32.82	342.2156/ 342.2157	C <sub>23</sub> H <sub>28</sub> F <sub>2</sub>
135734-59-7	 4-ethyl-4'-(4-(trifluoromethoxy)phenyl)-1,1'-bi(cyclohexyl)	32.89	354.21704/ 354.21705	C <sub>21</sub> H <sub>29</sub> F <sub>3</sub> O
133937-72-1	 4-Propyl-4'-[4-(trifluoromethoxy)phenyl]-1,1'-bi(cyclohexyl)	33.35	368.2326/ 368.2325	C <sub>22</sub> H <sub>31</sub> F <sub>3</sub> O
123560-48-5	 4-(4-Ethoxy-2,3-difluorophenyl)-4'-propyl-1,1'-bi(cyclohexyl)	33.47	364.2575/ 364.2575	C <sub>23</sub> H <sub>34</sub> F <sub>2</sub> O
97564-42-6	 4-propylphenyl 4-(4-propylcyclohexyl)cyclohexanecarboxylate	34.15	370.2870/ 370.2869	C <sub>25</sub> H <sub>38</sub> O <sub>2</sub>
133914-49-5	 4-pentyl-4'-[4-(trifluoromethoxy)phenyl]-1,1'-Bicyclohexyl	35.33	396.2639/ 396.2640	C <sub>24</sub> H <sub>35</sub> F <sub>3</sub> O

### 3.1.4. ICP-AES Analysis

Anionic, as well as cationic ions, usually present in trace amounts in LCs, can affect their electro-optical performance. Since recycled LC mixtures were recovered from an industrial extraction line, it is highly probable that a significant quantity of ions was incorporated. Therefore, qualitative and quantitative evaluation of the ions was crucial.

As expected, a large number of metal ions were found in the non-purified and purified LC mixtures, as presented in Table 2. With the exception of Ca, the concentrations of these unwanted ions obtained from the non-purified mixtures were higher than those from the purified mixtures. K and Na represent the elements with the highest amount. These ionic impurities present in the LC mixtures can originate from different sources during:

- their production process (even highly purified LCs possess ionic traces);
- the LCD manufacturing process (glue, alignment layers; filling could be a source of contamination);
- the aging process (chemical decomposition and degradation of LCs, charge transfer and electrochemical reactions in the electrodes);
- the dismantling of the LCD panels;
- the LC extraction process of the LCD panels on the industrial line (solubilization of the glue, polarizers, color filters, etc.).

**Table 2.** Qualitative and quantitative analysis of elements present in the non-purified and purified LC mixtures, determined by the ICP-AES technique. n.d. stands for “not determined”.

Element	NP-M1	NP-M2	NP-M3	Average	P-M1	P-M2	P-M3	Average
	(mg/L)-(ppm)							
Al	1.88	1.76	1.46	1.70 ± 0.11	2.06	1.43	1.40	1.63 ± 0.09
B	1.58	1.26	1.29	1.38 ± 0.05	0.32	0.46	0.36	0.38 ± 0.01
Ba	0.05	0.03	0.04	0.04 ± 0.01	0.019	0.012	0.011	0.013 ± 0.001
Be	0.20	0.18	0.19	0.19 ± 0.06	n.d.	n.d.	n.d.	n.d.
Ca	3.05	3.04	3.96	3.35 ± 0.24	3.42	3.89	3.57	3.63 ± 0.18
Cu	0.85	0.80	1.16	0.94 ± 0.05	n.d.	n.d.	n.d.	n.d.
Fe	1.34	1.09	1.35	1.26 ± 0.08	0.95	1.03	1.02	1.00 ± 0.06
K	28.73	23.38	29.57	27.23 ± 2.1	10.62	10.63	10.37	10.54 ± 0.55
Mg	2.05	1.01	2.57	1.88 ± 0.12	0.33	0.32	0.35	0.33 ± 0.01
Na	9.69	9.51	10.11	9.77 ± 0.60	4.63	4.58	3.82	4.34 ± 0.22
Sn	0.31	0.29	0.28	0.29 ± 0.01	0.210	0.290	0.250	0.25 ± 0.01
Sr	0.15	0.16	0.15	0.15 ± 0.01	0.05	0.04	0.05	0.050 ± 0.003
Ti	0.06	0.05	0.05	0.05 ± 0.01	0.038	0.020	0.020	0.026 ± 0.001
Zn	0.63	0.73	0.60	0.66 ± 0.03	0.21	0.29	0.25	0.25 ± 0.01

The results from the quantitative elementary analysis reported in this work reveal higher concentrations than those found in the literature by other authors [22]. Nevertheless, it should be pointed out that there are only few articles available, presenting an identification and, especially, a quantification of the ions (anions and cations) existing in the LC mixtures used for the manufacture of LCDs. Indirect methods were used to monitor the presence of ions in LCs. For example, resistivity measurements were performed during the LCD production process to perform quality control. The LC mixtures were then tested before and after insertion into the LCDs. Naemura et al. [22] and Liu et al. [23] used the ion chromatography technique to identify inorganic ions present in nematic LC (4-cyano-4'-

pentylbiphenyl). On the other hand, Hung et al. [24] analyzed ionic impurities using high resolution ICP-MS. Several ions reported by these authors [19] were also detected in the recycled LC mixtures studied in this work, with considerably higher concentrations. This result seems reasonable, since many other sources of contamination are present in the LC extraction process, as already mentioned above.

According to the results of the chemical characterization presented above, all studied LC mixtures exhibit quite comparable chemical properties. Therefore, only results from one non-purified (assigned NP) and one purified (P) LC mixture will be discussed in the following sections, to avoid redundancy.

### 3.2. Thermo-Optical and Thermal Properties

#### 3.2.1. TGA Analysis

Thermal stabilities of the non-purified and purified LC mixtures were studied using TGA in the temperature range comprised between 25 and 800 °C. Figure 5 presents the obtained two thermograms, exhibiting the mass loss as a function of increasing temperature. It can be deduced that the thermal decomposition followed a one-step degradation for all samples. This behavior indicates that, despite the presence of a large number of molecules in each LC mixture, these compounds degrade thermally in the same range of temperatures.

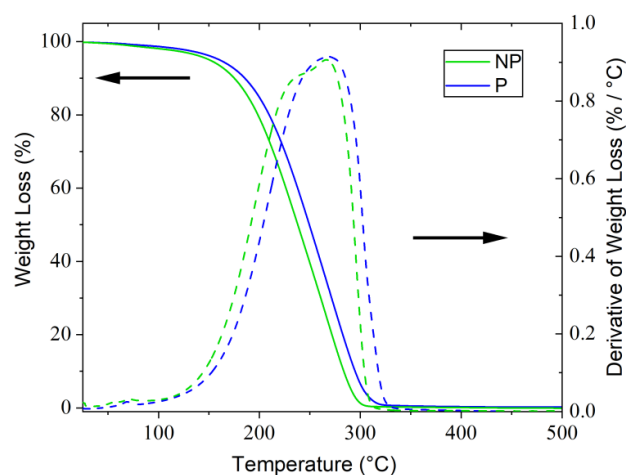


**Figure 5.** Thermograms of a non-purified and purified LC mixture in the temperature range between 25 and 100 °C, applying a heating rate of 10 °C/min. Dotted lines correspond to the derivatives of weight loss for each sample.

The obtained thermograms can be used to determine the thermal stability limit of the samples. This limit can be defined by the onset temperature  $T_{\text{onset}}$ , where the mass loss reaches 5%. According to Figure 5, all samples were thermally stable, up to temperatures of about 120 °C, and the final degradation temperature was observed around 255 °C. At the final temperature of the analysis (800 °C), the mass loss of all samples was close to 100%, confirming the absence of any inorganic species. As shown in Figure 5, the non-purified and the purified LC mixtures present the same thermal degradation behavior and do not exhibit considerable differences concerning their onset and final degradation temperatures.

#### 3.2.2. DSC Analysis

DSC analysis was performed to determine the phase transition temperatures and associated enthalpies. Figure 6 illustrates the thermograms obtained during heating and cooling cycles of a non-purified and a purified LC mixture.

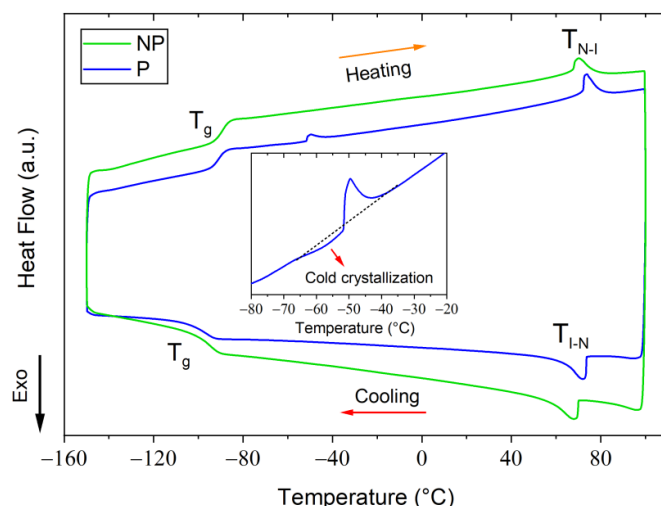


**Figure 6.** Thermograms obtained during heating and cooling cycles of non-purified and purified LC mixtures in the temperature range between  $-150$  and  $100$  °C, at a rate of  $10$  °C/min. The inset represents a zoom of the heating cycle near  $-50$  °C.

According to Figure 6, the thermograms of the non-purified and purified mixtures showed similar behavior during the heating cycle, as follows:

- around  $-90$  °C, a jump in the heat capacity of the samples was observed; this phenomenon can be assigned to a single glass transition ( $T_g$ ) of the LC molecules;
- the existence of a large homogeneous phase, between  $-90$  °C and  $70$  °C, which can be identified as nematic region from POM observations (see the following Section 3.2.3). The presence of this large nematic phase region extends the perspectives for future reuse and valorization opportunities;
- around  $70$  °C, an endothermic peak was detected, corresponding to a single nematic-isotropic transition ( $T_{N-I}$ ).

For all samples, the cooling cycle shows only the isotropic-nematic transition ( $T_{I-N}$ ) and the glass transition ( $T_g$ ). As expected, a slight shift towards lower temperatures was observed in cooling mode. Therefore, the behavior in heating and cooling modes was different. The values of the observed transitions temperatures and associated enthalpies are given in Table 3 for the heating cycle.

**Table 3.** Transition temperatures and associated enthalpies of non-purified and purified LC mixtures during a heating ramp, with a rate of  $10$  °C/min.

Sample	$T_g$ (°C)	$T_{LC_{ord}-N/melting}$ (°C)	$\Delta H_{LC_{ord}-N/melting}^*$ (J/g)	$T_{N-I}$ (°C)	$\Delta H_{N-I}$ (J/g)
Non-purified	$-90.0$	---	---	$71.2$	$2.1$
Purified	$-91.1$	$-50.1$	$0.59$	$73.6$	$2.5$

\* Enthalpy of cold crystallization (or/and ordering) for this purified mixture was  $0.22$  J/g.

An additional event was detected for the purified sample. Indeed, an endothermic peak was observed during the heating cycle at  $\sim -50$  °C, which could be related to the transition from a higher ordered LC phase to a lesser ordered LC phase ( $LC_{ord}-N$ ), or to the melting of an additional crystalline phase, or to a simultaneous evolution of these two phenomena [25–27]. Indeed, a zoom of this area (inset of Figure 6) revealed the presence of a weak exothermic peak starting around  $-60$  °C, which could be due to an effect of cold crystallization (or ordering), before the endothermic peak occurred. Since the enthalpies of these exo- and endo-thermic events were different, a superposition of the two above-mentioned phenomena might be assumed. Regarding the non-purified sample,

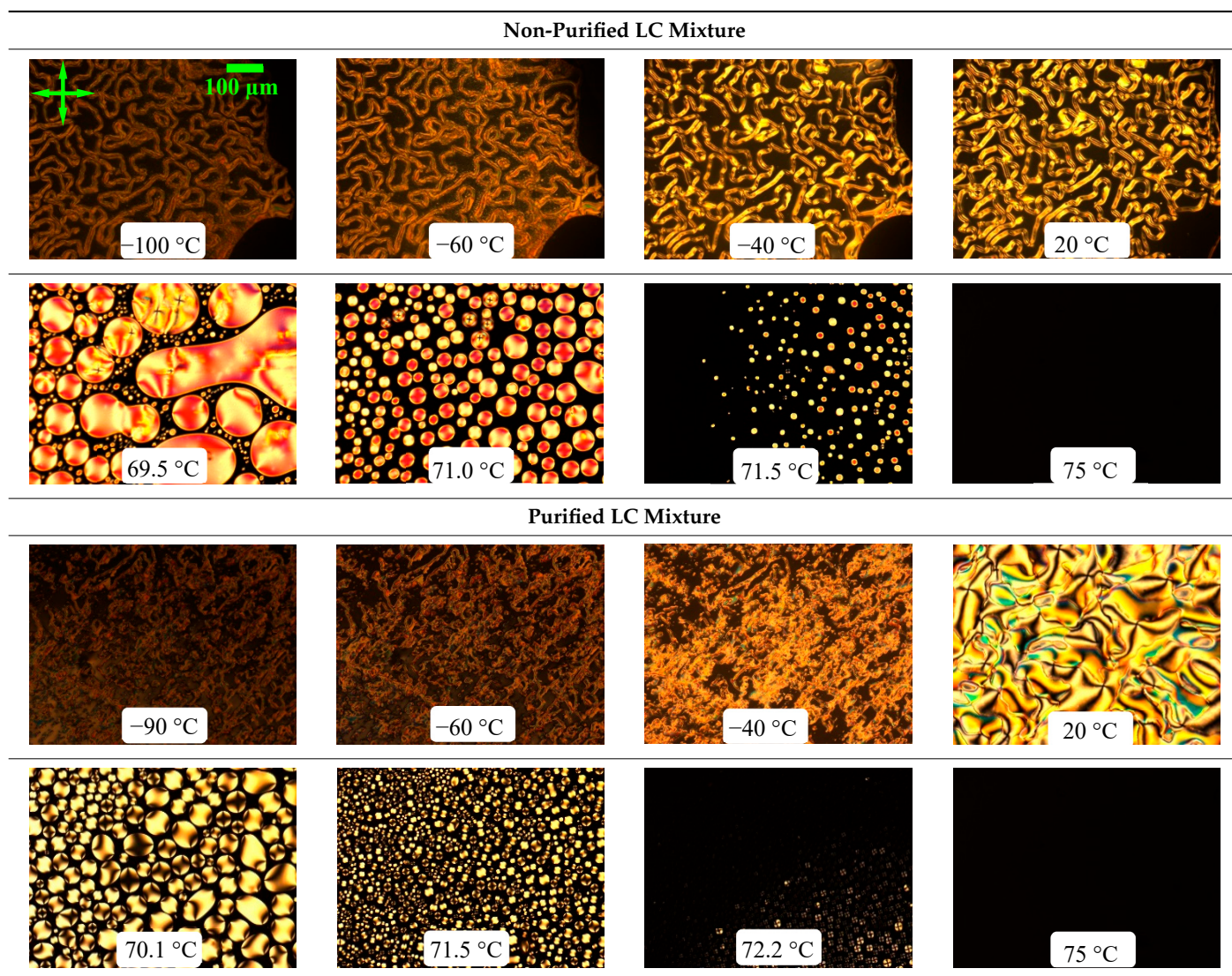


these particular events were not observed. POM and Wide-Angle X-ray scattering (WAXS) techniques were performed to further investigate this behavior (see the following sections).

### 3.2.3. POM Analysis

The POM analysis allowed for observation of the evolution of the sample morphologies of the LC mixtures, in order to identify the existing mesophases, and to determine the phase transitions of the compounds. The recorded textures of the non-purified and purified LC mixtures are displayed in Table 4. All images were captured with cross-polarizers, since the light through an LC sample is not quenched, as it is the case for an isotropic liquid.

**Table 4.** Textures of non-purified and purified LC mixtures observed by POM. The scale bar represents 100  $\mu\text{m}$  for all pictures. Measurements were taken with an X10/0.25 objective, using cross-polarizers, in a temperature range comprised between  $-100$  and  $90$   $^{\circ}\text{C}$ .



From a large panel of pictures taken at different temperatures, only eight have been selected for each sample. Observations were performed in heating mode to agree well with the sample treatment procedure applied for the DSC investigation.

Below the clearing point, all analyzed samples exhibited textures that can be attributed to nematic LCs. For non-purified and purified samples, at about  $-90$   $^{\circ}\text{C}$ , the recycled LC molecules appear to be frozen and quenched, showing a nematic glassy state (marbled textures). It is worth mentioning that the non-purified LC mixture exhibited a higher

number of inversion lines compared to the purified LC mixture. In the temperature range between  $-60$  and  $-40$  °C, the pictures show no textural change; therefore, it was not possible to contribute to the identification of the additional transition observed by DSC (around  $-50$  °C). This transition may be caused by a relatively small number of LC molecules compared to those confined in a dominant nematic domain, which could explain why this additional phenomenon was not observed by POM.

At room temperature, the LC molecules remain in the nematic state. Nevertheless, the nematic texture of the purified LC mixture has evolved, showing colored areas separated by black filaments known as Schlieren brushes [17]. These filaments correspond to an alignment of the LC molecules parallel to the axis of one or the other crossed polarizer, and, so, to an extinction position of the nematic state [28]. The non-purified sample retained the nematic marbled texture, with a large number of first-order inversion lines (thread-like texture), at low temperatures. The onset of the nematic-isotropic transition was observed at around  $70$  °C for the non-purified sample, and at  $72$  °C for the purified one. This shift, already detected for DSC experiments, was expected, since impurities might behave as “plasticizers” [29]. At  $75$  °C, the clearing point, corresponding to the nematic-isotropic transition temperature, was reached for both samples.

### 3.3. Wide-Angle X-ray Scattering

Wide-Angle X-ray (WAXS) diffractograms of the purified LC mixture obtained during heating and cooling ramps are presented in Figure 7. As described in Section 2.2.2, the sample was cooled from room temperature to its glassy state, followed by a heating cycle above the isotropic temperature, before undergoing a further cooling cycle. It can be noted that, at the same temperature, the diffraction patterns obtained during the two cooling cycles were perfectly reproducible and superimposable; therefore, only one cooling cycle is presented and will be discussed (Figure 7a).

In the isotropic state ( $T > 73.6$  °C), the LC moieties are all randomly distributed in space, implying that there is no long-range positional or orientation order within the molecules. The thermal fluctuations are important, and molecular motions seems not to be correlated. The X-ray patterns consist of two diffuse rings (Figure 7c). Indeed, even if no long-range order exists, a short-range positional order occurred, giving rise to two rings [30]. The large angle ring (centre of  $2\theta = 18.1^\circ$  at  $90$  °C) is related to the lateral distance between the molecules ( $d \sim 48.9$  nm), and the small angle ring ( $2\theta = 4.8^\circ$  at  $90$  °C) is linked to the longitudinal separation between mesogens ( $d \sim 184$  nm).

In the nematic phase ( $73.6 \geq T > -91.1$  °C), diffractograms and 2D X-ray patterns (Figure 7d) were found to be similar to those obtained for the isotropic state. However, the latter present a sharper intensity distribution and a slight  $2\theta$  shift. These phenomena were more prominent when the temperature decreased. To illustrate this, at  $72$  °C, the first peak is centered at  $18.3^\circ$  ( $d \sim 48.5$  nm), with a full-width at half-maximum (FWHM) of  $6.5^\circ$ , and the second one is centered at  $5.1^\circ$  ( $d \sim 172$  nm), with a FWHM of  $3.3^\circ$ . Meanwhile, at  $-72$  °C, the first peak is centered at  $19.8^\circ$  ( $d \sim 44.8$  nm), with a FWHM equal to  $4.1^\circ$ , whereas the second one is centered at  $5.4^\circ$  ( $d \sim 165$  nm), with a FWHM of  $0.9^\circ$ . It should be remembered that the nematic phase has a long-range orientation order, but no positional order. Therefore, the order parameter of the nematic phase increases with decreasing temperature, which explains why these peaks become thinner and sharper when lowering the temperature.



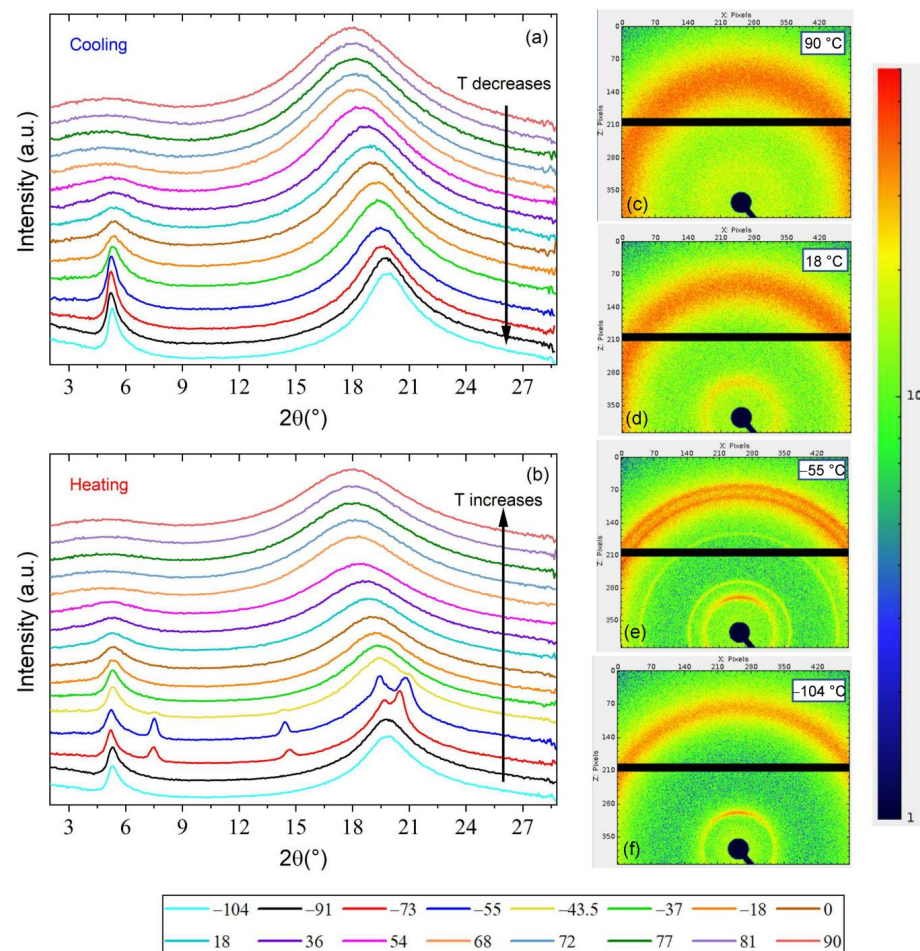


**Figure 7.** WAXS analysis of a purified LC mixture in the temperature range between  $-104$  and  $90$  °C, obtained with a rate of  $10$  °C/min: intensity versus  $2\theta$  obtained during the (a) cooling and (b) heating cycles. Two-dimensional X-ray patterns at: (c)  $90$  °C in the isotropic state (heating or cooling), (d)  $18$  °C in the nematic state (heating or cooling), (e)  $-55$  °C in the ordered phase, obtained only in heating mode, and (f)  $-104$  °C in the glassy state (heating or cooling).

In the glassy state ( $T \leq -91.1$  °C), the diffractograms were similar to those observed at higher temperatures in the nematic phase (Figure 7f).

During the heating cycle (Figure 7b), between  $-73$  and  $-43.5$  °C, three new sharp peaks appeared ( $2\theta = 7.5$ ,  $14.8$ , and  $20.5$ °, corresponding to  $d = 117.7$ ,  $59.8$  and  $43.3$  nm, respectively). These peaks could be related to the additional phase transition observed by DSC analysis in the same range of temperatures. The sharpness and the number of peaks may suggest either the presence of a crystalline phase, or a more ordered nematic or smectic phase [31]. For other temperatures, WAXS patterns obtained during the heating cycle overlapped with those from the cooling mode.

In terms of the phase changes, the set of diffraction patterns agreed well with the results obtained by DSC.

#### 4. Conclusions

In this work, three LC mixtures were investigated, corresponding to three consecutive recovery periods of 4-months in an industrial extraction line. At first, possible differences between non-purified and purified LC samples were established using chemical characterization techniques. FTIR,  $^1\text{H-NMR}$ , and GC-MS analysis of the non-purified and purified LC mixtures confirmed that their molecular structures, as well as their functional groups (aromatic rings, aliphatic chains, polar groups), corresponded well to those of typical LC molecules. The obtained spectra and chromatograms exhibited strong similarities between

non-purified and purified LC mixtures. However, the ICP-AES method revealed that a certain amount of inorganic impurities (ions) remained in the blends. These impurities can cause some adverse effects, such as an increase of the electrical conductivity, thus altering the electro-optical properties of the LCs.

In a subsequent step, thermal and thermo-optical properties of these mixtures were studied. Thermal (ATG, DSC) and thermo-optical (POM) analysis did not reveal significant differences between the non-purified and purified LC samples. For example, the temperatures corresponding to onset and end of the thermal degradation did not change, and were situated being ~150 and ~255 °C for all mixtures. Despite the presence of a large number of LC molecules, a single thermal decomposition step was observed for all samples. Textures of the LC mixtures obtained by POM observations confirm the typical Schlieren and marbled textures of nematic LC molecules. DSC analysis revealed a broad range of nematic phase between −90 and 70 °C, which is an important feature for their future reuse in LCD systems or other applications. In the temperature range between −60 and −50 °C, an additional phase transition was detected using DSC and WAXS techniques. However, the precise origin of this transition could not be well-identified. Even the POM analysis did not allow to observe a change in the textures in this temperature range.

All LC mixtures studied in this work showed similar chemical and thermal properties compared to conventional nematic LCs reported in the literature. Consequently, the reuse of such recycled nematic LC mixtures could be effective for devices operating at least between −50 and 70 °C.

**Author Contributions:** Conceptualization, U.M.; methodology, A.B. and U.M.; validation, A.B., C.B., C.F., P.S. and U.M.; investigation, A.B., B.O., C.B., F.D. (Florence Danede), F.D. (Frédéric Dubois) and J.-F.T.; data curation, A.B. and C.B.; writing—original draft preparation, A.B., C.B., C.F., F.D. (Frédéric Dubois), P.S. and U.M.; writing—review and editing, A.B., C.B., F.D. (Frédéric Dubois) and U.M. All authors have read and agreed to the published version of the manuscript.

**Funding:** This research was funded by the *Région Hauts-de-France* (FEDER), the I-Site of Lille, the Chevreur Institute (FR 2638), the Ministère de l'Enseignement Supérieur, de la Recherche et de l'Innovation, and the ENVIE<sup>2</sup>E du Nord company. The APC was funded by MDPI and by the University of Lille/France.

**Data Availability Statement:** The dataset presented in this study is available in this article.

**Acknowledgments:** The authors acknowledge financial support from the *Région Hauts-de-France* (FEDER), the I-Site of Lille, the Chevreur Institute (FR 2638), the Ministère de l'Enseignement Supérieur, de la Recherche et de l'Innovation, the ENVIE<sup>2</sup>E du Nord company, MDPI, and the University of Lille.

**Conflicts of Interest:** All authors declare no conflict of interest.

## References

1. Bressanelli, G.; Sacconi, N.; Pigosso, D.C.; Perona, M. Circular Economy in the WEEE industry: A systematic literature review and a research agenda. *Sustain. Prod. Consum.* **2020**, *23*, 174–188. [[CrossRef](#)]
2. Rene, E.R.; Sethurajan, M.; Ponnusamy, V.K.; Kumar, G.; Dung, T.N.B.; Brindhadevi, K.; Pugazhendhi, A. Electronic waste generation, recycling and resource recovery: Technological perspectives and trends. *J. Hazard. Mater.* **2021**, *416*, 125664. [[CrossRef](#)] [[PubMed](#)]
3. Azizi, D.D.S.; Hanafiah, M.M.; Woon, K.S. Material Flow Analysis in WEEE Management for Circular Economy: A Content Review on Applications, Limitations, and Future Outlook. *Sustainability* **2023**, *15*, 3505. [[CrossRef](#)]
4. Shittu, O.S.; Williams, I.D.; Shaw, P.J. Global E-waste management: Can WEEE make a difference? A review of e-waste trends, legislation, contemporary issues and future challenges. *Waste Manag.* **2021**, *120*, 549–563. [[CrossRef](#)] [[PubMed](#)]
5. Baldé, C.P.; D'Angelo, E.; Luda, V.; Deubzer, O.; Kuehr, R. *Global Transboundary E-Waste Flows Monitor 2022*; United Nations Institute for Training and Research: Bonn, Germany, 2022.
6. Li, J.; Su, G.; Letcher, R.J.; Xu, W.; Yang, M.; Zhang, Y. Liquid Crystal Monomers (LCMs): A New Generation of Persistent Bioaccumulative and Toxic (PBT) Compounds? *Environ. Sci. Technol.* **2018**, *52*, 5005–5006. [[CrossRef](#)] [[PubMed](#)]
7. Su, H.; Shi, S.; Zhu, M.; Crump, D.; Letcher, R.J.; Giesy, J.P.; Su, G. Persistent, bioaccumulative, and toxic properties of liquid crystal monomers and their detection in indoor residential dust. *Proc. Natl. Acad. Sci. USA* **2019**, *116*, 26450–26458. [[CrossRef](#)] [[PubMed](#)]

8. Cheng, Z.; Shi, Q.; Wang, Y.; Zhao, L.; Li, X.; Sun, Z.; Lu, Y.; Liu, N.; Su, G.; Wang, L.; et al. Electronic-Waste-Driven Pollution of Liquid Crystal Monomers: Environmental Occurrence and Human Exposure in Recycling Industrial Parks. *Environ. Sci. Technol.* **2022**, *56*, 2248–2257. [[CrossRef](#)] [[PubMed](#)]
9. Su, H.; Ren, K.; Li, R.; Li, J.; Gao, Z.; Hu, G.; Fu, P.; Su, G. Suspect Screening of Liquid Crystal Monomers (LCMs) in Sediment Using an Established Database Covering 1173 LCMs. *Environ. Sci. Technol.* **2022**, *56*, 8061–8070. [[CrossRef](#)] [[PubMed](#)]
10. Moundoungou, I.; Boubarka, Z.; Tabieguia, G.-J.F.; Barrera, A.; Derouiche, Y.; Dubois, F.; Supiot, P.; Foissac, C.; Maschke, U. End-of-Life Liquid Crystal Displays Recycling: Physico-Chemical Properties of Recovered Liquid Crystals. *Crystals* **2022**, *12*, 1672. [[CrossRef](#)]
11. Barrera, A.; Binet, C.; Dubois, F.; Hébert, P.-A.; Supiot, P.; Foissac, C.; Maschke, U. Dielectric Spectroscopy Analysis of Liquid Crystals Recovered from End-of-Life Liquid Crystal Displays. *Molecules* **2021**, *26*, 2873. [[CrossRef](#)] [[PubMed](#)]
12. Barrera, A.; Binet, C.; Dubois, F.; Hébert, P.-A.; Supiot, P.; Foissac, C.; Maschke, U. Recycling of Liquid Crystals From e-Waste. *Derivatives* **2022**, *21*, 55–61. [[CrossRef](#)]
13. Barrera, A.; Binet, C.; Dubois, F.; Hébert, P.-A.; Supiot, P.; Foissac, C.; Maschke, U. Temperature and frequency dependence on dielectric permittivity and electrical conductivity of recycled Liquid Crystals. *J. Mol. Liq.* **2023**, *378*, 121572. [[CrossRef](#)]
14. Collings, P.J.; Hird, M. *Introduction to Liquid Crystals: Chemistry and Physics*, 1st ed.; Taylor & Francis Ltd.: London, UK, 2017; ISBN 9781351989244.
15. Neyts, K.; Beunis, F. Ion Transport in Liquid Crystals. In *Handbook of Liquid Crystals*; Goodby, J.W., Tschierske, C., Raynes, P., Gleeson, H., Kato, T., Collings, P.J., Eds.; Wiley-VCH Verlag GmbH & Co. KGaA.: Weinheim, Germany, 2014; pp. 1–26.
16. Kawamoto, H. The History of Liquid-Crystal Display and Its Industry. In Proceedings of the 2012 Third IEEE HISToRY of ELeCtro-technology CONference (HISTELCON), Pavia, Italy, 5–7 September 2012; IEEE: Piscataway, NJ, USA; pp. 1–6.
17. Oswald, P.; Pieranski, P. *Nematic and Cholesteric Liquid Crystals*, 1st ed.; CRC Press: Boca Raton, FL, USA, 2005; ISBN 9780415321402.
18. Pawel, P.; Godinho, H.M. *Liquid Crystals: New Perspectives*, 1st ed.; John Wiley & Sons, Inc.: Hoboken, NJ, USA, 2021; ISBN 2013206534.
19. Lee, J.-H.; Liu, D.N.; Wu, S.T. *Introduction to Flat Panel Displays*, 1st ed.; John Wiley & Sons Ltd.: West Sussex, UK, 2008; ISBN 9780470516935.
20. Maschke, U.; Moundoungou, I.; Fossi-Tabieguia, G.J. Method for Extracting the Liquid Crystals Contained in an Element That Comprises a First Support and a Second Support—Associated Device. French Patent No. FR3017808 (A1); Patent No. EP3111276 (A1); Patent No. WO2015128582 (A1), 4 January 2017.
21. Kim, Y.; Lee, M.; Wang, H.S.; Ahn, S.; Kim, J.; Song, K. FTIR spectroscopic studies of polar nematic liquid crystals in various molecular arrangements. *Vib. Spectrosc.* **2017**, *92*, 182–187. [[CrossRef](#)]
22. Naemura, S.; Sawada, A. Ionic Conduction in Nematic and Smectic A Liquid Crystals. *Mol. Cryst. Liq. Cryst.* **2003**, *400*, 79–96. [[CrossRef](#)]
23. Liu, Y.; Mou, S. Ion chromatographic determination of some anions and alkaline cations in liquid crystal materials after ultraviolet irradiation. *Talanta* **2003**, *60*, 1205–1213. [[CrossRef](#)] [[PubMed](#)]
24. Hung, H.-Y.; Lu, C.-W.; Lee, C.-Y.; Hsu, C.-S.; Hsieh, Y.-Z. Analysis of metal ion impurities in liquid crystals using high resolution inductively coupled plasma mass spectrometry. *Anal. Methods* **2012**, *4*, 3631–3637. [[CrossRef](#)]
25. Jasiurkowska-Delaporte, M.; Rozwadowski, T.; Dmochowska, E.; Juszyńska-Gałązka, E.; Kula, P.; Massalska-Arodz, M. Interplay between Crystallization and Glass Transition in Nematic Liquid Crystal 2,7-Bis(4-pentylphenyl)-9,9-diethyl-9H-fluorene. *J. Phys. Chem. B* **2018**, *122*, 10627–10636. [[CrossRef](#)] [[PubMed](#)]
26. Ramos, J.J.M.; Diogo, H.P. Phase behavior and slow molecular dynamics in the glassy state and in the glass transformation of a nematic liquid crystal: 4CFPB. *Liq. Cryst.* **2020**, *47*, 604–617. [[CrossRef](#)]
27. Mansaré, T.; Decressain, R.; Gors, C.; Dolganov, V.K. Phase Transformations And Dynamics Of 4-Cyano-4'-Pentylbiphenyl (5cb) By Nuclear Magnetic Resonance, Analysis Differential Scanning Calorimetry, And Wideangle X-Ray Diffraction Analysis. *Mol. Cryst. Liq. Cryst.* **2002**, *382*, 97–111. [[CrossRef](#)]
28. Davis, E.J.; Goodby, J.W. Classification of Liquid Crystals According to Symmetry. In *Handbook of Liquid Crystals: 8 Volume Set*; Goodby, J.W., Collings, J., Kato, T., Tschierske, C., Gleeson, H., Raynes, P., Vill, V., Eds.; Wiley-VCH Verlag GmbH & Co. KGaA.: Weinheim, Germany, 2014; pp. 27–56; ISBN 3527327738.
29. Bukowczan, A.; Hebda, E.; Pielichowski, K. The influence of nanoparticles on phase formation and stability of liquid crystals and liquid crystalline polymers. *J. Mol. Liq.* **2021**, *321*, 114849. [[CrossRef](#)]
30. Agra-Kooijman, D.M.; Kumar, S. X-Ray Scattering Investigations of Liquid Crystals. In *Handbook of Liquid Crystals: 8 Volume Set*; Goodby, J.W., Collings, J., Kato, T., Tschierske, C., Gleeson, H., Raynes, P., Vill, V., Eds.; Wiley-VCH Verlag GmbH & Co. KGaA.: Weinheim, Germany, 2014; pp. 301–338; ISBN 3527327738.
31. Gray, G.W.; Goodby, J.W.C. *Smectic Liquid Crystals: Textures and Structures*, 1st ed.; Leonard Hill: Oakland, CA, USA, 1984; ISBN 0863440258.

**Disclaimer/Publisher's Note:** The statements, opinions and data contained in all publications are solely those of the individual author(s) and contributor(s) and not of MDPI and/or the editor(s). MDPI and/or the editor(s) disclaim responsibility for any injury to people or property resulting from any ideas, methods, instructions or products referred to in the content.